RSC Advances

PAPER

View Article Online
View Journal | View Issue

Cite this: *RSC Adv.*, 2020, **10**, 12395

Poly(3,4-ethylenedioxyselenophene): effect of solvent and electrolyte on electrodeposition, optoelectronic and electrochromic properties†‡

Preeti Yadav,[ab] Sheerin Naqvi[ab] and Asit Patra *[ab]

In this article, we report the effect of electropolymerization conditions such as solvent and supporting electrolyte on the redox, optoelectronic and electrochromic properties of PEDOS. Monomer EDOS was synthesized by new and simple route and its electropolymerization was investigated by employing six different combinations of solvent–electrolyte namely $TBAClO_4$/MeCN, $TBAPF_6$/MeCN, $TBABF_4$/MeCN, $TBAClO_4$/PC, $TBAPF_6$/PC and $TBABF_4$/PC. Further, the electrochemical, spectroelectrochemistry, morphology and electrochromic properties of resultant PEDOS films were systematically studied. A pronounced effect of both solvent and supporting electrolyte on the electropolymerization, redox, optoelectronic and electrochromic properties on PEDOS film is noted. Among all solvent–electrolyte systems, MeCN and $TBAClO_4$ were found to be the most suitable medium for electropolymerization of EDOS. Further, PEDOS films prepared in PC showed red shifted absorption maxima, narrow absorption peaks in UV-vis-NIR spectra, slightly more smooth morphologies, and high optical contrasts ratio and coloration efficiency in comparison to MeCN. PEDOS films prepared in $TBABF_4$/PC exhibited longer λ_{max} (670 nm), smooth morphology, and the highest optical contrasts ratio (44.6%) and coloration efficiency (141.8 $cm^2\ C^{-1}$) compared to the other solvent–electrolyte medium.

Received 14th February 2020
Accepted 12th March 2020

DOI: 10.1039/d0ra01436b

rsc.li/rsc-advances

1. Introduction

Since the discovery of high electrical conductivity in doped polyacetylene,[1] many conjugated polymers[2] have been developed as active components for application in organic electronic devices such as organic field effect transistors,[3,4] organic photovoltaics,[5,6] organic light emitting diodes,[7] electrochromic devices[8,9] and sensors,[10,11] *etc.*[12] Among various conjugated polymers, polythiophene and its derivatives,[13,14] namely poly(3,4-ethylenedioxythiophene) (PEDOT),[15,16] have proved to be the most promising organic electronic materials owing to their excellent physical and chemical properties. Indeed, the good electrochemical and thermal stability of PEDOT, moderate band gap (1.6 eV), high optical transparency in the doped state, high electrical conductivity and low oxidation potential have resulted in its widespread application in variety of electronic and optoelectronic devices.[17,18] Recently, two dimensional polymers and materials have emerged as promising candidate for designing of multifunctional materials with better electronic and optoelectronic properties.[19]

In contrast to polythiophene and PEDOT, their selenium analogue have drawn attention only in recent years[20,21] despite possessing better properties such as narrow band gap, low redox potential, better charge transport and higher doping. Yet, very few groups have paid attention to the development and study of selenophene derivatives for organic electronics.[22,23] In particular, the extensive computational and experimental work on oligo and polyselenophenes by Bendikov's group is quite significant in understanding the chemistry of selenophene based conjugated systems.[24–28] Compared to the extensive research focussed on EDOT relatively little is known about the electrochemical study of 3,4-ethylenedioxyselenophene (EDOS) based conjugated polymers. In particular, most of the efforts are mainly devoted in achieving better chemical and optoelectronic properties of poly(3,4-ethylenedioxyselenophene) (PEDOS) by structural modification such as by introducing substituents on the ethylenedioxy bridge or alkyl groups, incorporation of heteroatom or by chemical copolymerization.[29] Cihaner and coworkers studied the electrochromic performance of electropolymerized naphthalenylmethyl-substituted 3,4-propylenedioxyselenophene (ProDOS) derivatives.[30] Xu and coworkers reported the electrochemical synthesis of alkylated ProDOS in ionic liquid[31] and EDOS in microemulsion system with water and studied their electrochromic properties.[32] Most recently, our group reported the electropolymerization of EDOS on

[a]*Photovoltaic Metrology Section, Advanced Materials & Device Metrology Division, CSIR-National Physical Laboratory, Dr. K. S. Krishnan Marg, New Delhi-110012, India. E-mail: apatra@nplindia.org*

[b]*Academy of Scientific and Innovative Research (AcSIR), Ghaziabad-201002, India*

† In memory of Prof. Michael Bendikov.

‡ Electronic supplementary information (ESI) available. See DOI: 10.1039/d0ra01436b

flexible substrate and examined the effect of electrode surface on the electrochemical, spectroelectrochemical and electrochromic performance of PEDOS films.[33]

It is known that electrochemical and optical properties of polymer films are considerably influenced by electropolymerization conditions such as solvent and supporting electrolyte. However, few studies have focussed on the correlation of optical and electrochemical properties of polymer films with electropolymerization conditions. Indeed, some groups have studied the effect of polymerization conditions on the nucleation and polymer growth and provided a correlation between experimental parameters of electropolymerization with morphologies, optical and redox properties of conjugated polymers. For example, Bendikov and coworkers systematically studied the role of solvent and supporting electrolyte on the morphology and electro-optical properties of PEDOT and demonstrated that solvent has a major effect on the properties while electrolyte has only minor effect.[34] Lu and coworkers reported that poly(thieno[3,4-*b*]-1,4-oxathiane) showed better electroactivity, compact morphology and better electrochromic properties for film polymerized in $BmimPF_6$ compared to CH_2Cl_2-$BmimPF_6$ and CH_2Cl_2-$TBAPF_6$.[35] Xu and coworkers studied the effect of polymerization solvent on the electrochemical, morphological and electrochromic properties of nitrogen analogue of PEDOT, poly(*N*-methyl-3,4-dihydrothieno [3,4-*b*][1,4]oxazine) (PMDTO).[36] Arteaga and coworkers reported the effect of supporting electrolyte on the conductivity, morphology and electrochemical polymerization of PEDOT.[37] Zhao and coworkers reported the electropolymerization of 3-methylselenophene in three different electrolytic medium and studied the redox, morphology and optoelectronic properties of poly(3-methylselenophene).[38]

Compared to numerous study on the effect of electropolymerization conditions on the properties of PEDOT,[39] PEDOS has not been investigated in sufficient details considering its advantages over PEDOT. Indeed, a systematic and detailed study on the effect of solvent and supporting electrolyte on the electrochemical and optical properties of PEDOS is still limited to only one report till date. During preparation of this manuscript, we came across the article describing the effect of electrolyte media on electropolymerization and optical properties of PEDOS films by Xu and coworkers.[40] Nevertheless, experimental conditions in this study are limited to polymerization in CH_2Cl_2-$TBAPF_6$, CH_2Cl_2-$BmimPF_6$ and $BmimPF_6$. Moreover, this study uses ionic liquid as media for polymerization which has limitations of poor solubility and high viscosity. Yet, despite this effort, fundamental study on electropolymerization of EDOS in conventional organic solvents and commonly used supporting electrolytes to provide a comprehensive understanding of the electrochemical behaviour, morphology and optical properties of the resultant PEDOS films is much needed for its various applications and has a significant scope for development.

Herein, we present a systematic study on the influence of solvents and supporting electrolytes on the electrochemical behaviour of EDOS in different media to obtain PEDOS films with better electrochemical and optoelectronic properties. We report the electropolymerization of EDOS in conventional organic solvents acetonitrile (MeCN) and propylene carbonate (PC) in presence of three commonly used supporting electrolytes, namely tetrabutylammonium perchlorate ($TBAClO_4$), tetrabutylammonium hexafluorophosphate ($TBAPF_6$) and tetrabutylammonium tetrafluoroborate ($TBABF_4$). Further, a detailed study on the effect of solvent–electrolyte system on polymerization, electrochemical properties, spectroelectrochemistry, morphology and electrochromic performance of six resultant PEDOS film is also presented followed by a throughout comparison. Monomer EDOS was synthesized by a simple and alternative route.

2. Experimental section

2.1 Chemicals

Selenophene, bromine (Br_2), anhydrous methanol (MeOH), copper(II) oxide (CuO) and anhydrous ethanol (EtOH) were purchased from Sigma-Aldrich. Zinc powder (Zn), acetic acid (AcOH), hydrochloric acid (HCl), potassium iodide (KI), ethylene glycol and toluene were purchased from Sisco Research Laboratories, Mumbai, India. For chromatography separations, columns were prepared using silica gel (mesh size 60–230). $TBAClO_4$, $TBAPF_6$, $TBABF_4$ were purchased from Sigma-Aldrich and dried under vacuum before use. MeCN and PC were obtained from Sigma-Aldrich. All the materials were used as received without any purification unless otherwise mentioned.

2.2 Instrumentation

UV absorption spectra were recorded using UV1800 Shimadzu spectrophotometer. ^1H and ^{13}C NMR spectra were recorded in $CDCl_3$ using tetramethylsilane as external standard. All electrochemical measurements were performed using Metrohm Autolab PGSTAT204 potentiostat in conventional three-electrode cell using Pt disk or indium tin oxide (ITO) coated glass slide as working electrode, Au wire as counter electrode and Ag/Ag^+ as reference electrode. Prior to each electrochemical studies, solution was purged with nitrogen to remove any oxygen. PEDOS films were obtained by electropolymerization of 0.01 M EDOS in solvents (MeCN and PC) using supporting electrolytes ($TBAClO_4$, $TBPF_6$ and $TBABF_4$) over 10–15 cycles at 100 mV s^{-1}. After polymerization, PEDOS films were rinsed with MeCN to remove electrolyte and residual monomers before their electrochemical, optical and morphology study. Spectroelectrochemical and electrochromic studies of PEDOS films (deposited on ITO coated glass slides, dimensions (8 mm × 50 mm × 1.1 mm, $R_s < 10\ \Omega\ sq^{-1}$)) were performed in monomer free same solvent–electrolyte media as used for deposition of polymer films. Surface morphologies of the polymer films deposited in different solvent–electrolyte media were investigated by scanning electron microscopy (SEM). SEM images of PEDOS films were obtained using modal Zeiss EVO MA10. For morphology studies, PEDOS films of similar polymerization charges were prepared in different solvent–supporting

electrolyte media by multisweep electropolymerization of 0.01 M EDOS.

2.3. Synthesis of 3,4-ethylenedioxyselenophene

2.3.1 Synthesis of 2,3,4,5-tetrabromoselenophene (2). To a well stirred solution of selenophene (**1**) (1.40 g, 10.69 mmol) in $CHCl_3$ (20 mL) and AcOH (1.5 mL), Br_2 (10.7 g, 3.40 mL) was added dropwise at 0 °C over a period of 1 h. The resulting reaction mixture was stirred for 12 h at room temperature followed by reflux for another 6 h in oil bath. After completion of the reaction, the resulting reaction mixture was allowed to cool to room temperature and transferred to a large beaker. Excess Br_2 was evaporated and the crude residue was diluted with $CHCl_3$ (30 mL). The organic phase was washed with water (3 × 25 mL), once with brine (20 mL), dried over $MgSO_4$ and concentrated under reduced pressure. The crude product tetrabromoselenophene (**2**) was purified by column chromatography using hexane as eluent to yield white crystals in 75% yield (3.57 g). ^{13}C NMR (62.5 MHz, $CDCl_3$) δ 117.9, 112.2.

2.3.2 Synthesis of 3,4-dibromoselenophene (3). Zn powder (0.88 g, 13.45 mmol) was added in small portions to a refluxing solution of tetrabromoselenophene (2.0 g, 4.48 mmol) in a mixture of EtOH (10.2 mL), AcOH (2.5 mL) and 0.1 mL of HCl (11.97 N) over 5 min. After refluxing for 3 h, the reaction mixture was filtered hot and upon cooling to room temperature concentrated. The crude residue was diluted with CH_2Cl_2. The combined organic layers were washed with water (3 × 25 mL), brine (20 mL) and dried over anhydrous $MgSO_4$ and concentrated under reduced pressure. Purification of crude product by column chromatography using hexane as eluent afforded oil **3** in 60% yield (0.77 g). ^{1}H NMR (250 MHz, $CDCl_3$) δ 7.93 (s, 2H) ^{13}C NMR (62.5 MHz, $CDCl_3$) δ 127.4, 114.3.

2.3.3 Synthesis of 3,4-dimethoxyselenophene (4). To a solution of 3,4-dibromoselenophene (**3**) (1.0 g, 3.47 mmol) in anhydrous MeOH (12 mL), sodium methoxide (16.3 mmol, prepared by dissolving 376 mg Na in MeOH), CuO (0.69 g, 8.67 mmol) and KI (115 mg, 0.69 mmol) were added successively. The resulting mixture was heated to reflux for 3 days under nitrogen atmosphere. After completion of the reaction, residue was filtered and washed with $CHCl_3$ (25 mL). Organic layer was concentrated and crude residue was washed with water. Aqueous layer was extracted with diethyl ether (3 × 25 mL), washed once with brine (20 mL), dried over $MgSO_4$ and concentrated. Crude product was purified using column chromatography using a mixture of hexane and ethyl acetate (40 : 1 ratio) to yield colourless oil in 71% yield (0.47 g) that solidified after storage at low temperature. ^{1}H NMR (250 MHz, $CDCl_3$) δ 6.56 (s, 2H), 3.86 (s, 6H) ^{13}C NMR (62.5 MHz, $CDCl_3$) δ 148.9, 96.0, 57.0.

2.3.4 Synthesis of 3,4-ethylenedioxyselenophene (5). To a solution of 3,4-dimethoxyselenophene (**4**) (250 mg, 1.32 mmol) in toluene (80 mL), ethylene glycol (0.5 mL, 7.93 mmol) and *p*-toluenesulphonic acid (*p*TSA) (60 mg) were added and the resulting reaction mixture was heated at 60 °C for 6 h. After completion of the reaction, residue was diluted with ethyl acetate. The combined organic layer was washed with water (3 × 25 mL), once with brine (20 mL), dried over $MgSO_4$ and concentrated. Crude product was purified by column chromatography using a mixture of hexane and ethyl acetate in 20 : 1 ratio. EDOS was obtained as a colourless oil in 48% yield (0.12 g).^{1}H NMR (250 MHz, $CDCl_3$) δ 6.78 (s, 2H), 4.16 (s, 4H), ^{13}C NMR (62.5 MHz, $CDCl_3$) δ 142.7, 101.7, 64.3.

3. Results and discussion

3.1 Monomer synthesis

The monomer EDOS was synthesized by a new and simple route for electropolymerization as presented in Scheme 1.[41] EDOS was firstly prepared by Aqad and group using a five-step synthetic methodology similar to the industrial synthetic route of EDOT.[42] We had previously reported, a much simpler synthetic strategy to prepare EDOS from 2,3-dimethoxy-1,3-butadiene and selenium dichloride in two steps.[25] Zade and coworkers synthesized EDOS from trimethylsilylated diyne using zirconocene dichloride and selenium dichloride.[43] However, these two synthetic schemes suffer from the usage of selenium dichloride which is toxic in nature and inhibited further study. Herein, we have synthesized EDOS from selenophene (**1**) by a simple route. Compound **1** was subjected to bromination using liquid bromine to obtain 2,3,4,5-tetrabromoselenophene (**2**) which was then selectively debrominated at 2 and 5-position using Zn-AcOH to yield 3,4-dibromoselenophene (**3**). Compound **3** on treatment with freshly prepared sodium methoxide afforded 3,4-dimethoxyselenophene (**4**) as a colorless oil. In the final

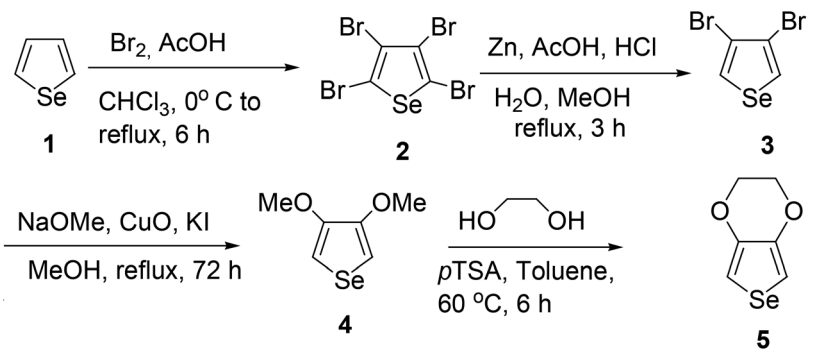

Scheme 1 Synthesis route of 3,4-ethylenedioxyselenophene (**5**).

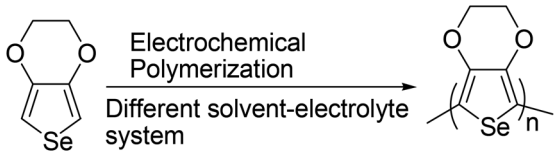

Scheme 2 Electrochemical polymerization of EDOS in different solvent–electrolyte media.

step, compound **4** was transetherificated using ethylene glycol in presence of acid catalyst to give 3,4-ethylenedioxyselenophene (EDOS; **5**). Compound **5** was stored at low temperature and found to be stable for over years.

3.2 Electropolymerization in different solvent–electrolyte media

In order to investigate the effect of polymerization media on the electropolymerization, electrochemical and optical properties of the resultant polymer PEDOS, monomer EDOS (0.01 M) was electrodeposited by repetitive cycling on Pt electrode in different solvent–electrolyte media at 100 mV s^{-1} for 10 cycles (Scheme 2). We carried out the electrochemical polymerization in the presence of three supporting electrolytes consisting of different counter anions *viz* $TBAClO_4$, $TBAPF_6$ and $TBABF_4$ and two solvent namely MeCN and PC. The first anodic oxidation curve of EDOS in different solvent–electrolyte systems is shown in Fig. 1 and data is summarized in Table 1. Oxidation of EDOS in MeCN was initiated at 1.09 V in $TBAClO_4$, 1.10 V in $TBAPF_6$ and 1.13 V in $TBABF_4$. However in PC, EDOS was oxidized at 1.06 V in $TBAClO_4$, 1.11 V in $TBAPF_6$ and 1.07 V in $TBABF_4$. These results clearly indicate that the oxidation potential of monomer in both solvents MeCN and PC are almost identical whereas a noticeable difference is observed in the case of supporting electrolytes.

The multisweep elctropolymerization of EDOS in different solvent–electrolyte media is shown in Fig. 2. As shown in Fig. 2a, upon repetitive potential scanning of monomer EDOS in $TBAClO_4$/MeCN between −1.0 V and 1.3 V, a broad redox wave was generated in the region −0.7 to 0.9 V which corresponds to redox behaviour of electrodeposited polymer PEDOS. This is attributed to the formation of polymers with broad chain length distribution and conversion of the conductive species from neutral to oxidized states. An increase in current density upon repetitive cycling suggests a gradual deposition of polymer films onto the electrode surface. A slight shift in cathodic and anodic peak potentials indicated the increased electrical resistance of the polymer films and therefore requires slightly high potential to overcome this. This behaviour is characteristic of conjugated polymers during electropolymerization.[44–46] A similar result was found during electropolymerization of EDOS in other solvent–electrolyte media.

The polymerization behaviour of EDOS is found to be different in different solvent–electrolyte media. Increment in current density per cycle was found to be comparatively higher in MeCN than PC which clearly suggests better polymerization efficiency in MeCN. However, a more uniform current

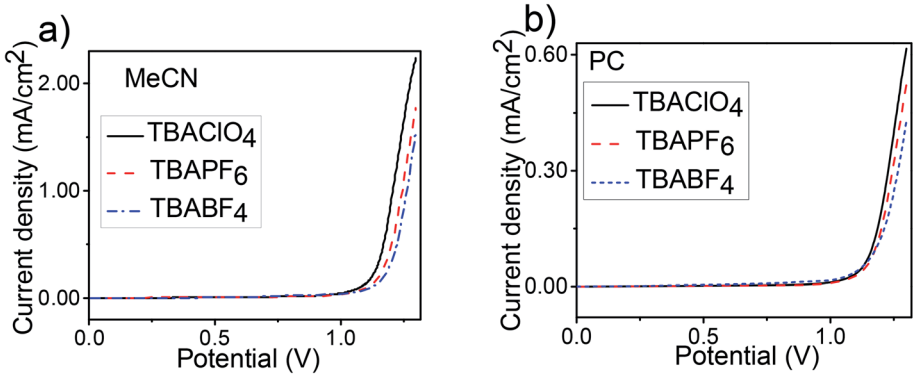

Fig. 1 First anodic oxidation curve of EDOS on Pt electrode in different solvent–electrolyte media (a) MeCN (b) PC at scan rate of 100 mV s^{-1}.

Table 1 Oxidation potential of monomer EDOS and current increment during electropolymerization in different solvent–electrolyte media

Solvent–electrolyte media	E^{ox}_{onset} (V)	Average current increment per cycle (mA cm^{-2})	Current increment (mA cm^{-2})	
			Between 1st and 2nd cycle	Between 9th and 10th cycle
$TBAClO_4$/MeCN	1.09	0.060	0.033	0.067
$TBAPF_6$/MeCN	1.10	0.049	0.038	0.051
$TBABF_4$/MeCN	1.13	0.042	0.023	0.056
$TBAClO_4$/PC	1.06	0.016	0.010	0.017
$TBAPF_6$/PC	1.11	0.015	0.011	0.015
$TBABF_4$/PC	1.07	0.014	0.010	0.015

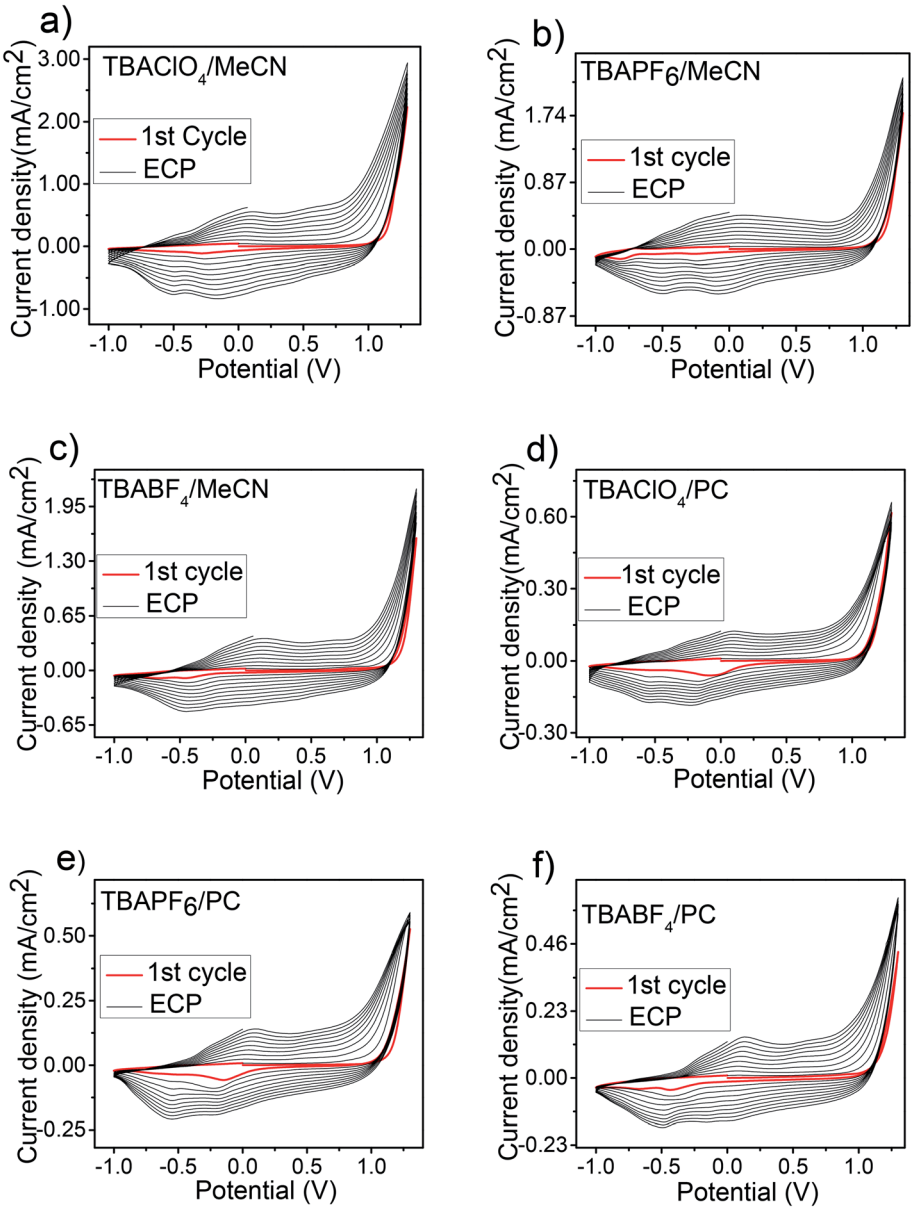

Fig. 2 Multisweep electropolymerization of 0.01 M EDOS on Pt electrode in (a) $TBAClO_4$/MeCN, (b) $TBAPF_6$/MeCN, (c) $TBABF_4$/MeCN, (d) $TBAClO_4$/PC, (e) $TBAPF_6$/PC and (f) $TBABF_4$/PC at scan rate of 100 mV s^{-1}.

increment from cycle to cycle was observed in case of PC compared to MeCN. A significant difference of counter anions on polymerization efficiency was also noted. When $TBAClO_4$ was used as supporting electrolyte, polymerization efficiency was found to be better compared to $TBAPF_6$ and $TBABF_4$ as indicated by significantly high current increment in case of $TBAClO_4$. We observed that current increment between 9th and 10th cycle was higher than 1st and 2nd cycle indicating a higher deposition rate of polymer on the electrode surface in final cycle. As presented in Table 1, the current increment indicates the gradual increase in polymer deposition rate upon successive cycling.

The different electrochemical behaviour of EDOS during electropolymerization is mainly explained by difference in nature of solvents and counter anions as all other experimental parameters such as monomer concentration, number of cycles and potential sweep rate were same. Better polymerization efficiency of EDOS observed in MeCN compared to PC is explained by difference of dielectric constant and viscosity (see ESI, Table S1‡). Due to high dielectric constant of PC, oligomers of short-chain length formed during the initial stage of polymerization solubilize readily leading to slow deposition of polymer films on the electrode surface. Moreover, high viscosity of PC also slows down the speed of monomer and oligomers during electropolymerization.[34,36] This indicates that MeCN is more suitable medium for polymerization of EDOS as compared to PC similar to previously reported polymerization behaviour of MDTO[36] and terthiophene.[47]

In addition to solvent, electropolymerization of EDOS is also influenced by supporting electrolyte. The different polymerization efficiency observed in case of supporting electrolytes is attributed to difference in nature of anions, since cation (tetrabutylammonium) is same in all the cases. Efficient polymerization in case of $TBAClO_4$ compared to $TBAPF_6$ and $TBABF_4$ is due to high mobility of ClO_4^- as compared to PF_6^- and BF_4^- which results in high current increment indicating better polymerization efficiency.[48] During polymerization process, formation of polaron–anion pair takes place which leads to the immobalization of counter anions inside the polymer matrix. Since an anion with high mobility will be replaced more rapidly by monomers during polymerization and consequently better polymerization efficiency in case of $TBAClO_4$.[48,49] These results clearly demonstrate that both solvent and supporting electrolyte have significant effect on the electropolymerization of EDOS, but the effect of solvent is more pronounced as compared to the electrolyte. We conclude that for electropolymerization of EDOS, MeCN and $TBAClO_4$ were found to be a more efficient solvent and electrolyte respectively compared to other solvent–electrolyte media used in this study.

3.3 Electrochemistry of PEDOS films

The redox behaviour of the PEDOS films prepared from different solvent–electrolyte media were investigated by cyclic voltammetry (CV) in monomer-free solvent–electrolyte system to evaluate their electrochemical properties. As shown in

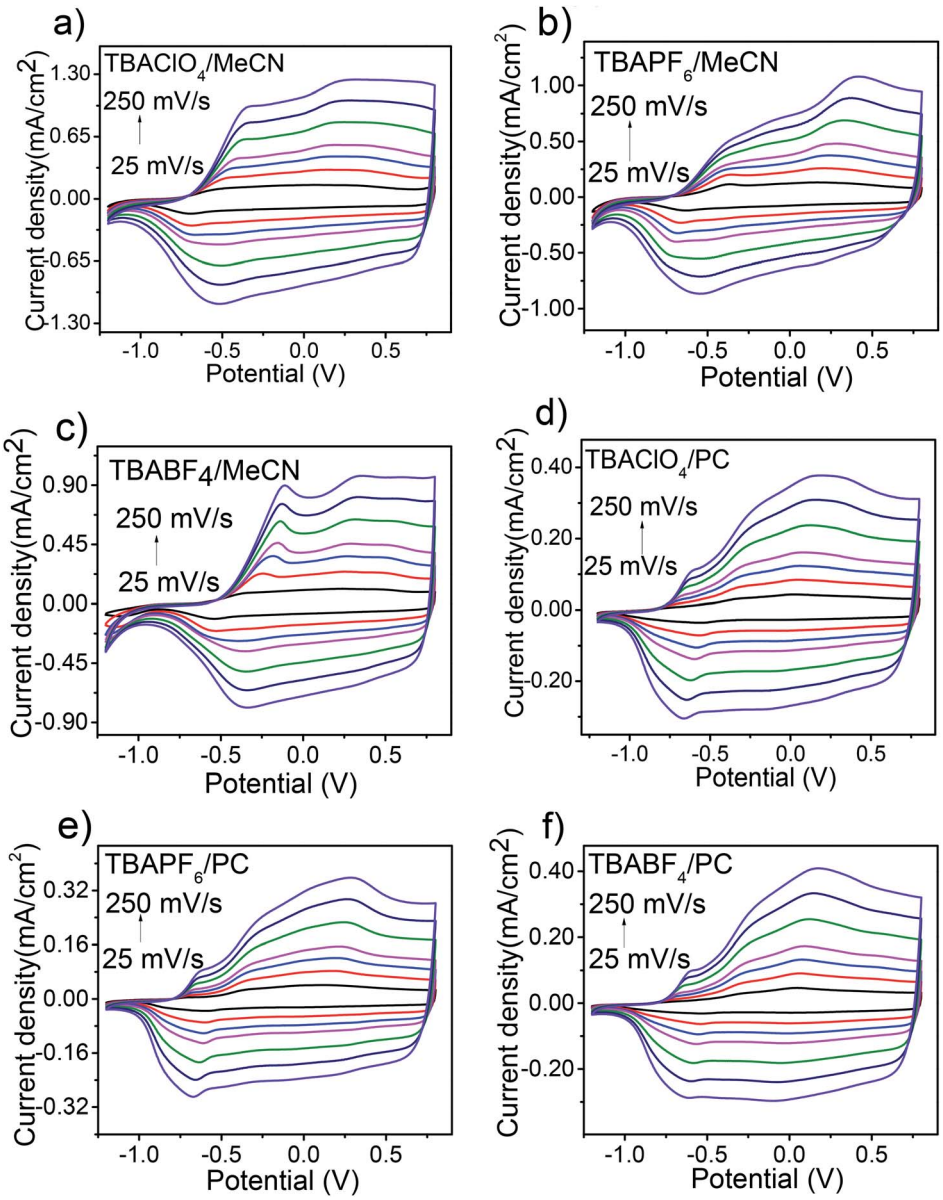

Fig. 3 Cyclic voltammograms of PEDOS films prepared in different media recorded in monomer free solvent–electrolyte systems (a) $TBAClO_4$/MeCN, (b) $TBAPF_6$/MeCN, (c) $TBABF_4$/MeCN, (d) $TBAClO_4$/PC, (e) $TBAPF_6$/PC and (f) $TBABF_4$/PC at scan rates of 25, 50, 75, 100, 150, 200 and 250 mV s^{-1}.

Table 2 The redox properties of PEDOS polymerized in different solvent–electrolyte media

Solvent–electrolyte media	$E^{ox}_{poly,onset}$ (V)	Q_{Oxid}[a] (μC cm^{-2})	Q_{Red}[b] (μC cm^{-2})	Q_{Oxid}/Q_{Red}
$TBAClO_4$/MeCN	−0.68	84.7	77.0	1.10
$TBAPF_6$/MeCN	−0.65	64.8	58.9	1.10
$TBABF_4$/MeCN	−0.52	61.3	54.0	1.13
$TBAClO_4$/PC	−0.77	23.6	22.4	1.05
$TBAPF_6$/PC	−0.74	21.0	20.5	1.02
$TBABF_4$/PC	−0.72	23.5	22.6	1.04

[a] Oxidation charges. [b] Reduction charges.

Fig. 3, CV of PEDOS films in all the solvent–electrolyte media at different scan rates showed broad redox peaks (cathodic and anodic), and significant hysteresis in cathodic and anodic peak potentials. This may be attributed to slow, non-homogeneous electron transfer and slow interconversion between redox species during the redox process.[50] Furthermore, a linear dependence between scan rates and peak current in case of all solvent–electrolyte system showed that the redox process is non-diffusion controlled with polymer films being well adhered to the surface of working electrode (Fig. S1‡). In all solvent–electrolyte media, the ratio between Q_{Oxid} and Q_{Red} for PEDOS film was found to be close to 1 or slightly higher which indicates a good reversibility of redox processes.

It was observed that films prepared in different solvent–electrolyte media showed different electroactivity. PEDOS films prepared in MeCN were oxidized at comparatively high potential and exhibited more well-defined oxidation and reduction peaks than films obtained in PC. This difference in the electrochemical behaviour due to solvents is explained by slow and smooth growth of longer polymer chains in PC which results in faster electron transfer.[36,51] A similar trend was noticed in the CV of PMDTO films prepared in MeCN and PC.[36] It is noteworthy to mention that the redox behaviour of PEDOS films were also considerably influenced by supporting electrolytes. The oxidation potential of polymer film prepared and characterized in $TBABF_4$ was slightly high in comparison to those obtained in the case of $TBAClO_4$ and $TBAPF_6$ in both the solvents MeCN and PC (Table 2). This might be attributed to the high mobility of ClO_4^- and PF_6^- which results in easy migration inside the polymer matrix for charge compensation during oxidation process while for BF_4^- incomplete doping occurs (as a result of high nucleophilcity of BF_4^- it is more solvated by solvent molecules which hinders its mobility into polymer matrix)[52] resulting in high oxidation level as compared to ClO_4^- and PF_6^-.[48]

3.4 Spectroelectrochemical characterization of PEDOS films

The optoelectronic properties of PEDOS films prepared in different solvent–electrolyte media were investigated using UV-vis-NIR absorption spectroscopy. The UV-vis-NIR absorption spectra of PEDOS films in oxidized and neutral states were recorded under different applied potential in the same electrolyte–solvent systems as used for the preparation of films. It was noted that monomer EDOS shows similar absorption maxima in MeCN (λ_{max} 269 nm) and PC (λ_{max} 271 nm) (Fig. S2‡). The spectroelectrochemical data of PEDOS films recorded in different media is shown in Fig. 4 and summarized in Table 3. As shown in Fig. 4a, the absorption spectra of PEDOS film in neutral state at −0.9 V using $TBAClO_4$/MeCN medium exhibits absorption maxima at 648 nm originating from π–π* transitions. Upon successive increase of potential from −0.9 to 0.5 V (neutral to doped state), intensity of the π–π* transition gradually decreases with shift of absorption maxima to NIR region owing to the formation of polarons and bipolarons in the doped state along the polymer backbone. A similar trend was followed in the absorption spectra of PEDOS films prepared in other solvent–electrolyte media as well. Consequently, changes in absorption spectra were also accompanied with colour change from deep blue in neutral state to colourless in doped (oxidized) state in all solvent–electrolyte media. It is noteworthy to mention that both solvent and supporting electrolyte used for polymerization has considerable effect on absorption spectra of polymer films. However, effect of solvent on absorption spectra of PEDOS is more predominant in comparison to supporting electrolytes.

The absorption spectra of PEDOS films prepared in PC are red-shifted as compared to MeCN (Fig. S3‡). In case of PEDOS films prepared in PC using $TBAClO_4$, $TBAPF_6$ and $TBABF_4$, absorption maxima are red-shifted by 4 nm, 10 nm, 47 nm, respectively *versus* films deposited in MeCN. Furthermore, absorption spectra in PC are slightly narrow in comparison to MeCN as indicated by their full width half maximum (FWHM) values. This difference in absorption spectra of the films prepared in PC and MeCN is explained by high dielectric constant and viscosity of PC. It has been mentioned in literature that oligomers of short-chain length have high solubility in PC due to its high dielectric constant than MeCN.[34,36] During the polymerization process, short oligomers solubilize readily in PC as compared to MeCN resulting in the formation of long-chain length polymers and thereby producing a sharp UV spectrum with longer absorption wavelength. Moreover, high dielectric constant of PC also reduces the resistivity of the solution during electropolymerization, leading to more smooth film formation. While deposition of oligomers of short-chain lengths in MeCN onto the electrode surface leads to high nucleation centres and results in the formation of polymer films with broad distribution of chain length and high surface roughness. This results in

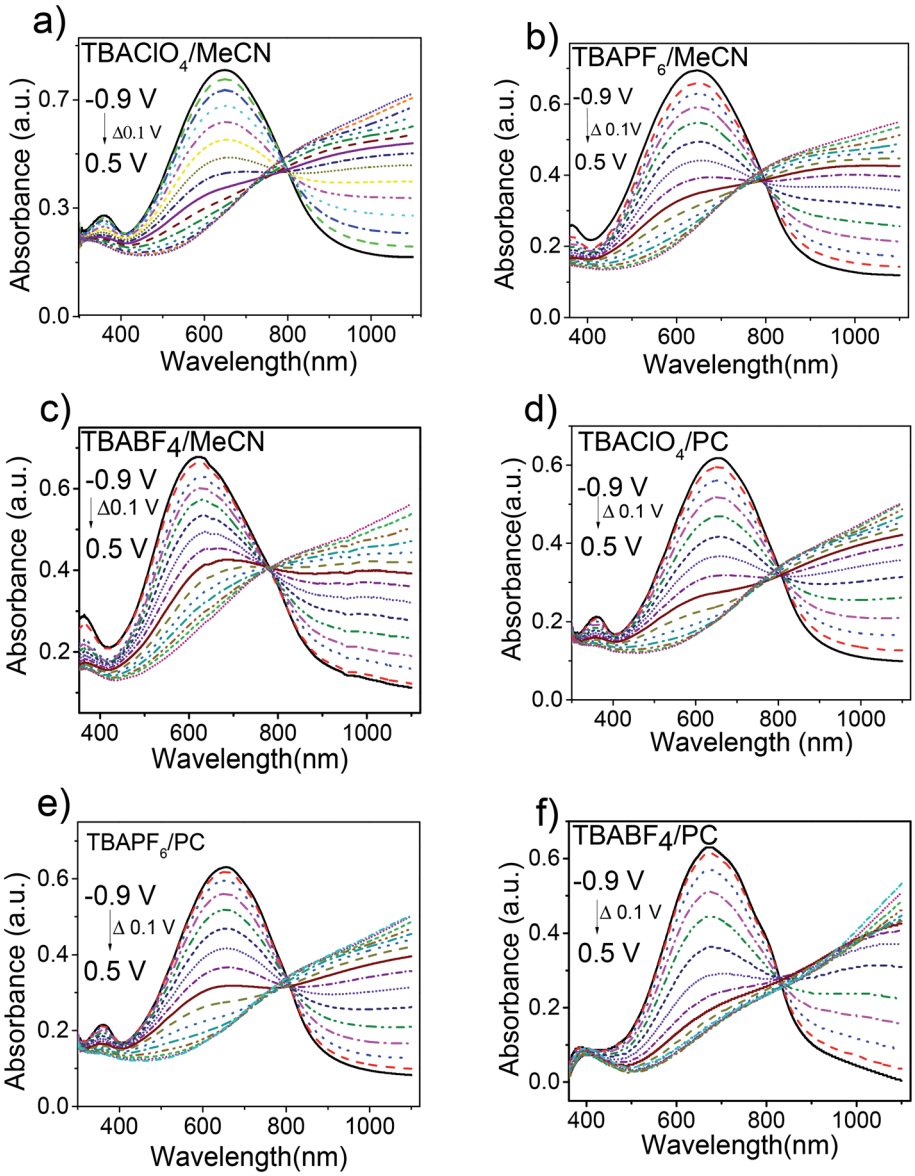

Fig. 4 Spectroelectrochemistry of PEDOS films in monomer free solvent–electrolyte media on ITO coated glass substrate at different applied potentials in (a) $TBAClO_4$/MeCN, (b) $TBAPF_6$/MeCN, (c) $TBABF_4$/MeCN, (d) $TBAClO_4$/PC, (e) $TBAPF_6$/PC and (f) $TBABF_4$/PC.

broad absorption spectra and shorter wavelength maxima for films prepared in MeCN as compared to PC similar to PEDOT and PMDTO.[34,36]

Interestingly, supporting electrolyte has also substantial effect on the absorption maxima of PEDOS films (Fig. S4‡). It was noted that absorption maxima in case of $TBABF_4$ is blue-

Table 3 Spectroelectrochemical data of PEDOS films prepared in different solvent–electrolyte media

Solvent–electrolyte media	UV-vis absorption			
	λ_{max}[a] (nm)	λ_{onset}[b] (nm)	FWHM[c] (nm), [eV]	Band gap (eV)
$TBAClO_4$/MeCN	648	893	259 [0.78]	1.38
$TBAPF_6$/MeCN	644	885	255 [0.78]	1.40
$TBABF_4$/MeCN	623	890	250 [0.77]	1.39
$TBAClO_4$/PC	652	890	251 [0.74]	1.39
$TBAPF_6$/PC	654	887	245 [0.73]	1.39
$TBABF_4$/PC	670	886	237 [0.64]	1.39

[a] Wavelength determined at absorption peak maximum of polymer in neutral (dedoped) state. [b] Wavelength calculated from onset of the absorption peak of polymer in neutral state. [c] FWHM determined from absorption peak of polymer in neutral state.

shifted in MeCN, as compared to $TBAPF_6$ and $TBAClO_4$. In contrast to this, absorption maxima of PEDOS film in $TBABF_4$ is red shifted in PC than $TBAPF_6$ and $TBAClO_4$. Moreover, FWHM values are also significantly affected by supporting electrolytes in MeCN. It is noteworthy to mention that the absorption onset of the PEDOS films prepared in different media is unaffected similar to that observed for PEDOT.[34] Overall, absorption spectra of PEDOS films is significantly affected by both solvents and supporting electrolytes. However, the effect of solvent is more predominant on optical properties as compared to supporting electrolyte, with $TBABF_4$ being an exception.

3.5 Electrochromic properties

Further, the electrochromic properties of PEDOS films such as optical contrasts ratio ($\Delta T\%$), response time and coloration efficiency were investigated using chronoabsorptometry technique. Polymer films were switched alternatively between oxidized and neutral states upon switching the potential from −0.9 V to 0.5 V at λ_{max} with a residence time of 5 s. For the study of electrochromic parameters, PEDOS films were prepared in different solvent–electrolyte system by repetitive cyclic voltammetry of EDOS. Switching studies were performed in the same solvent–electrolyte media as that used for the deposition of polymer films.

Fig. 5 and Table 4 summarizes the optical switching data of polymers prepared in different solvent–electrolyte media at λ_{max}. It was noted that all polymers exhibit high transmittance in the doped state irrespective of solvent–electrolyte media used for the preparation of films. A significant change in optical contrasts ratio of PEDOS films was observed in both solvent and

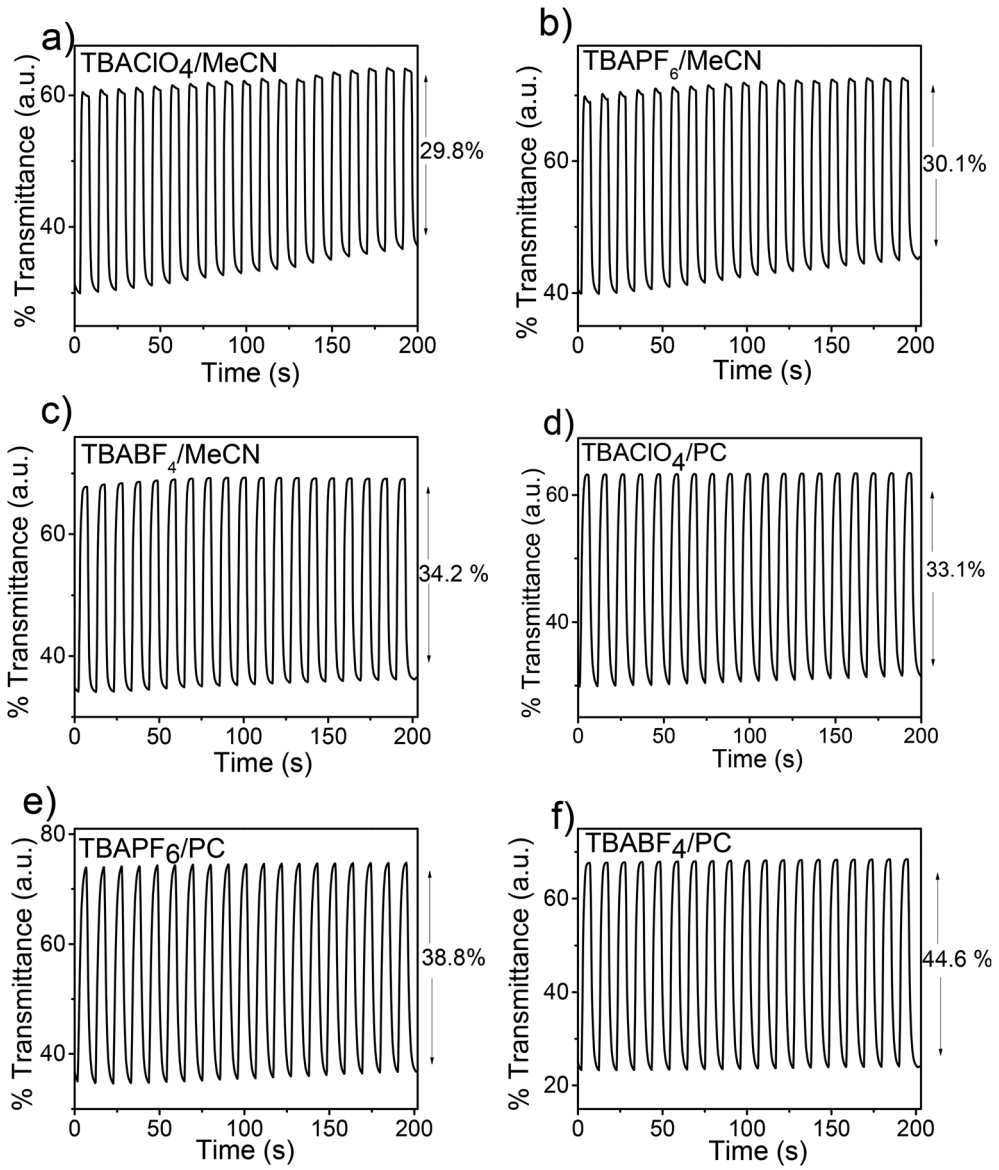

Fig. 5 Transmittance time profiles of PEDOS films obtained by switching the films between −0.9 to 0.5 V at time interval of 5 s in different solvent–electrolyte system.

Table 4 Electrochromic performance of PEDOS films prepared in different solvent–electrolyte media

Solvent–electrolyte media	Wavelength (nm)	$\Delta T\%$	Response time[a] (s) τ_{oxi}	CE[b] ($cm^2\ C^{-1}$)	Injected charge density (mC cm^{-2})
$TBAClO_4$/MeCN	648	29.8	0.8	81.6	3.51
$TBAPF_6$/MeCN	644	30.1	1.5	67.1	3.55
$TBABF_4$/MeCN	623	34.2	2.0	90.7	3.25
$TBAClO_4$/PC	652	33.1	2.0	97.4	3.28
$TBAPF_6$/PC	654	38.8	2.6	104.5	3.08
$TBABF_4$/PC	670	44.6	2.5	141.8	3.26

[a] Response time calculated at 95% of full switch from neutral to doped state. [b] Coloration efficiency (CE) is calculated by $CE = \log(T_{Oxid}/T_{Red})/$ injected charge density, where T_{oxid} refers to transmittance in doped state and T_{Red} refers to transmittance in dedoped state.[53]

electrolyte media. Nonetheless, the effect of solvent is more prominent as compared to supporting electrolyte, but considerable difference of supporting electrolytes on electrochromic properties were also observed in PC *versus* MeCN. PEDOS films prepared in PC showed better optical contrasts ratio as observed in case of MeCN. It is also noted that though supporting electrolytes have only a small effect on $\Delta T\%$ of PEDOS films in MeCN, but considerable difference was observed in PC. Indeed, $\Delta T\%$ of PEDOS films prepared in PC was significantly higher compared to those obtained in MeCN. PEDOS film prepared in $TBABF_4$/PC shows the highest contrasts ratio of 44.6% and coloration efficiency 141.8 $cm^2\ C^{-1}$ compared to other solvent–electrolyte systems. These results are found to be in good correlation with absorption spectra. High optical contrasts ratio observed in PC can be explained by its high dielectric constant than MeCN. As mentioned previously that high solubility of short oligomers in PC during the electropolymerization results in the formation of polymers of long-chain length and longer absorption maxima. Whereas in case of MeCN, oligomers of short-chain lengths are present that cannot be switched under the switching conditions used for PEDOS with long chains. In addition to this, deposition of short oligomers on electrode surface also leads to high nucleation centres resulting in films with high roughness. This results in poor electrochromic performance of films in MeCN.[34,36] In contrary to optical contrasts ratio, PEDOS films in PC showed longer response time in comparison to those obtained in MeCN. This is mainly due to high viscosity of PC which apparently reduces the mobility of counter ions than in case of MeCN. In case of films prepared and analysed in MeCN, slightly longer response time was noticed in case of $TBABF_4$ (2.0 s) and $TBAPF_6$ (1.4 s) than $TBAClO_4$ (0.8 s). This behaviour might be explained by the high mobility of ClO_4^- as compared to BF_4^- and PF_6^- which facilitates the easy migration of ClO_4^- ions during the doping and dedoping process and reduces τ_{oxi}.

3.6 Morphology study

In order to further investigate the effect of polymerization conditions on the surface morphology and to obtain a correlation between structure and optical properties of the resultant PEDOS films, their surface morphologies were studied using SEM. The surface morphologies of the polymer films prepared in different medium is shown in Fig. S5.‡ It was observed that both solvent and supporting electrolyte has only a minor effect on the surface morphologies of PEDOS films. PEDOS films prepared in PC have slightly smooth and uniform morphologies as compared to films prepared in MeCN. This observation is similar to previous reports that polymerization in PC provides film with smooth, homogeneous distribution of particles and flat morphology than films prepared in MeCN.[34,36] This is explained by high polarity of PC which favours the solubility of short oligomers resulting in homogeneous growth of polymer films on the electrode surface.[51] Moreover, high viscosity of PC results in slow diffusion of species (monomer, oligomers and counter anions) during polymerization limiting the polymerization rate as compared to MeCN. This indicates the formation of polymer films with more ordered structure due to slow process for film growth resulting in smooth and compact morphology.[34,36,51] It was noted that films prepared using $TBABF_4$ showed more compact structure and smooth morphologies as compared to films prepared using $TBAPF_6$ and $TBAClO_4$. It is also important to mention that PEDOS film prepared using $TBABF_4$/PC has more smooth morphology as compared to other solvent–electrolyte media. This result seems to correlate well with enhanced optical properties that is both longer absorption maxima and better electrochromic properties of PEDOS prepared using $TBABF_4$/PC. Consequently, morphology studies clearly indicate that properties of PEDOS films are clearly influenced by polymerization conditions such as solvent and supporting electrolyte.

4. Conclusions

In summary, we have electrodeposited PEDOS films with different redox and optoelectronic properties from EDOS monomer by using six different combinations of solvent–electrolyte media. EDOS was synthesized by a simple and alternative route. It was noted that both solvent and supporting electrolyte used for polymerization have significant influence on the electropolymerization, redox, optoelectronic and electrochromic properties of the resultant PEDOS films. However compared to solvent, supporting electrolyte has only a moderate effect on the properties of PEDOS films. We found that MeCN and $TBAClO_4$ are the most efficient solvent–electrolyte media for electropolymerization of EDOS. Electrochemical study revealed that PEDOS films obtained in PC were oxidized at comparatively

lower potential than MeCN while for electrolytes the order $E_{TBABF_4} > E_{TBAPF_6} > E_{TBAClO_4}$ is followed. Further investigation of morphologies and optical properties revealed that appropriate selection of solvent and supporting electrolyte can be used to control optoelectronic and electrochromic properties. Optical and SEM studies suggested that though MeCN was found to be more efficient solvent medium for polymerization, films prepared in PC demonstrated more smooth morphologies, better optoelectronic and electrochromic properties. This is attributed to high dielectric constant and viscosity of PC which provides a better environment for polymer growth during polymerization resulting in deposition of more homogeneous films as compared to MeCN. Among all solvent–electrolyte media, PEDOS film prepared in $TBABF_4$/PC medium exhibited longest absorption maxima (λ_{max} 670 nm), highest optical contrasts ratio (44.6%) and coloration efficiency (141.8 cm^2 C^{-1}). Further study on electropolymerization of EDOS in the aqueous system and behaviour of the resulting PEDOS films are under process.[54]

Conflicts of interest

There are no conflicts to declare.

Acknowledgements

P.Y. is thankful to CSIR-New Delhi for her fellowship.

References

1 C. K. Chiang, Y. W. Park, A. J. Heeger, H. Shirakawa, E. J. Loius and A. G. MacDiramid, *J. Chem. Phys.*, 1978, **69**, 5098–5104.
2 T. A. Skotheim, *Handbook of Conducting Polymers, Marcel Dekker*, New York, 1998.
3 P. Gao, D. Beckmann, H. N. Tsao, X. Feng, V. Enkelmann, W. Pisula and K. Mullen, *Chem. Commun.*, 2008, **13**, 1548–1550.
4 Z. Chen, H. Lemke, S. Albert-Seifried, M. Caironi, M. M. Nielsen, M. Heeney, W. Zhang, I. McCulloch and H. Sirringhaus, *Adv. Mater.*, 2010, **22**, 2371–2375.
5 (*a*) J. Nelson, *Mater. Today*, 2011, **14**, 462–470; (*b*) G. Li, W. H. Chang, Y. Yang, G. Li, W. H. Chang and Y. Yang, *Nat. Rev. Mater.*, 2017, **2**, 17043.
6 A. Facchetti, *Chem. Mater.*, 2010, **2**, 3733–3758.
7 (*a*) P. K. Bhatnagar, *Organic Light-Emitting Diodes—A Review Nanomaterials and Their Applications*, Springer, Singapore, 2018; (*b*) J. Gao, *Curr. Opin. Electrochem.*, 2018, **7**, 87–94.
8 J. Sun, Y. Chen and Z. Liang, *Adv. Funct. Mater.*, 2016, **26**, 2783–2799.
9 T. W. Neo, Q. Ye, S. J. Chua and J. Xu, *J. Mater. Chem. C*, 2016, **4**, 7364–7376.
10 S. Inal, J. Rivnay, A. O. Suiu, G. G. Malliaras and I. McCulloch, *Acc. Chem. Res.*, 2018, **51**, 1368–1376.
11 Y. Lyu and K. Pu, *Adv. Sci.*, 2017, **4**, 1600481.
12 S. Singhal, P. Yadav, S. Naqvi, S. Gupta and A. Patra, *ACS Omega*, 2019, **4**, 3484–3492.
13 (*a*) V. Agrawal, Shahjad, D. Bhardwaj, R. Bhargav, G. D. Sharma, R. K. Bjardwaj, A. Patra and S. Chand, *Electrochimica Acta*, 2016, **192**, 52–60; (*b*) A. Mishra, C.-Q. Ma and P. Bäuerle, *Chem. Rev.*, 2009, **109**, 1141–1276.
14 I. F. Perepichka and D. F. Perepichka, *Handbook of Thiophene-based Materials: Applications in Organic Electronics and Photonics*, John Wiley & Sons, 2009, vol. 2.
15 J. Roncali, P. Blanchard and P. Frere, *J. Mater. Chem.*, 2005, **15**, 1589–1610.
16 L. B. Groenendaal, G. Zotti, P.-H. Aubert, S. M. Waybright and J. R. Reynolds, *Adv. Mater.*, 2003, **15**, 855–879.
17 L. B. Groenendaal, F. Jonas, D. Freitag, H. Pielartzik and J. R. Reynolds, *Adv. Mater.*, 2000, **12**, 481–494.
18 R. Vhargav, D. Bhardwaj, Shahjad, A. Patra and S. Chand, *ChemistrySelect*, 2016, **1**, 1347–1352.
19 (*a*) L.-M. Yang, I. A. Popov, T. Frauenheim, A. I. Boldyrev, T. Heine, V. Bačić and E. Ganz, *Phys. Chem. Chem. Phys.*, 2015, **17**, 26043–26048; (*b*) J.-H. Liu, Y.-M. Yang and E. Ganz, *RSC Adv.*, 2019, **9**, 27710–27719; (*c*) L.-M. Yang, V. Bačić, I. A. Popov, A. I. Boldyrev, T. Heine, T. Frauenheim and E. Ganz, *J. Am. Chem. Soc.*, 2015, **137**, 2757–2762; (*d*) J.-H. Liu, L.-M. Yang and E. Ganz, *J. Mater. Chem. A*, 2019, **7**, 3805–3814; (*e*) Q. Zhang, H. Dong and W. Hu, *J. Mater. Chem. C*, 2018, **6**, 10672–10686; (*f*) P. Payamyar, B. T. King, H. C. Öttinger and A. D. Schlüter, *Chem. Commun.*, 2016, **52**, 18–34.
20 (*a*) I. Kang, T. K. An, J.-A. Hong, H.-J. Yun, R. Kim, D. S. Chung, C. E. Park, Y.-H. Kim and S.-K. Kwon, *Adv. Mater.*, 2013, **25**, 524–528; (*b*) Z. Chen, H. Lemke, S. Albert-Seifried, M. Caironi, M. M. Nielsen, M. Heeney, W. Zhang, I. McCulloch and H. Sirringhaus, *Adv. Mater.*, 2010, **22**, 2371–2375.
21 (*a*) A. Patra and M. Bendikov, *J. Mater. Chem.*, 2010, **20**, 422–433; (*b*) A. Patra and M. Bendikov, in Selenium- and tellurium-containing organic π-conjugated oligomers and polymers, *Patai's Chemistry of Functional Groups, vol. 3, part 1*, ed. Z. Rappaport, Wiley, New York, 2012, pp. 523–584.
22 A. Patra, M. Bendikov and S. Chand, *Acc. Chem. Res.*, 2014, **47**, 1465–1474.
23 (*a*) X. He and T. Baumgartner, *RSC Adv.*, 2013, **3**, 11334–11350; (*b*) A. Patra, R. Kumar and S. Chand, *Isr. J. Chem.*, 2014, **54**, 621–641; (*c*) J. Hollinger, D. Gao and D. S. Seferos, *Isr. J. Chem.*, 2014, **54**, 440–453.
24 A. Patra, Y. H. Wijsboom, G. Leitus and M. Bendikov, *Chem. Mater.*, 2011, **23**, 896–906.
25 A. Patra, Y. H. Wijsboom, S. S. Zade, M. Li, Y. Sheynin, G. Leitus and M. Bendikov, *J. Am. Chem. Soc.*, 2008, **130**, 6734–6736.
26 M. Li, A. Patra, Y. Sheynin and M. Bendikov, *Adv. Mater.*, 2009, **21**, 1707–1711.
27 A. Patra, V. Agrawal, R. Bhargav, Shahjad, D. Bhardwaj, S. Chand, Y. Sheynin and M. Bendikov, *Macromolecules*, 2015, **48**, 8760–8764.
28 M. Li, Y. Sheynin, A. Patra and M. Bendikov, *Chem. Mater.*, 2009, **2**, 2482–2488.

29 Y. H. Wijsboom, Y. Sheynin, A. Patra, N. Zamoshchik, R. Vardimon, G. Leitus and M. Bendikov, *J. Mater. Chem.*, 2011, **21**, 1368–1372.
30 B. Karabey, L. C. Pekel and A. Cihaner, *Macromolecules*, 2015, **48**, 1352–1357.
31 W. Zhang, W. Zhang, S. Chen, B. Guo, H. Gu, Y. Xue, Z. Xue and J. Xu, *J. Electroanal. Chem.*, 2019, **833**, 17–25.
32 W. Zhang, W. Zhang, H. Liu, N. Jian, K. Qu, S. Chen and J. Xu, *J. Electroanal. Chem.*, 2018, **813**, 109–115.
33 P. Yadav, S. Singhal and A. Patra, *Synth. Met.*, 2020, **260**, 116264.
34 E. Poverenov, M. Li, A. Bitler and M. Bendikov, *Chem. Mater.*, 2010, **22**, 4019–4025.
35 Z. Wang, J. Xu, B. Lu, S. Zhang, L. Qina, D. Mo and S. Zhen, *Langmuir*, 2014, **30**, 15581–15589.
36 S. Ming, Z. Feng, D. Mo, Z. Wang, K. Lin, B. Lu and J. Xu, *Phys. Chem. Chem. Phys.*, 2016, **18**, 5129–5138.
37 M. A. del Valle, A. M. Ramírez, L. A. Hernández, F. Armijo, F. R. Díaz and G. C. Arteaga, *Int. J. Electrochem. Sci.*, 2016, **11**, 7048–7065.
38 B. Lu, S. Zhen, S. Ming, J. Xu and G. Zhao, *RSC Adv.*, 2015, **5**, 70649–70660.
39 (*a*) M. Ates, T. Karazehir, F. Arican and N. Eren, *J. Coat. Technol. Res.*, 2013, **10**, 317–330; (*b*) C. Li and T. Imae, *Macromolecules*, 2004, **37**, 2411–2416; (*c*) L. Zhang, Y. Wen, Y. Yao, X. Duan, J. Xu and X. Wang, *J. Appl. Polym. Sci.*, 2013, 2660–2670.
40 K. Qu, H. Liu, N. Jian, B. Lu, A. Liu and J. Xu, *Int. J. Electrochem. Sci.*, 2019, **14**, 7884–7898.
41 https://lib-phds1.weizmann.ac.il/Dissertations/Wijsboom_Yair_33542002.pdf.
42 E. Aqad, M. V. Lakshmikantham and M. P. Cava, *Org. Lett.*, 2001, **3**, 4283–4285.
43 S. Das, P. K. Dutta, S. Panda and S. S. Zade, *J. Org. Chem.*, 2010, **75**, 4868–4871.
44 G. Q. Shi, J. K. Xu and M. X. Fu, *J. Phys. Chem. B*, 2002, **106**, 288–292.
45 J. K. Xu, J. Hou, S. S. Zhang, G. M. Nie, S. Z. Pu, L. Shen and Q. Xiao, *J. Electroanal. Chem.*, 2005, **578**, 345–355.
46 B. Dong, Y. H. Xing, J. K. Xu, L. Q. Zheng, J. Hou and F. Zhao, *Electrochim. Acta*, 2008, **53**, 5745–5751.
47 A. Sezai Sarac, U. Evans, M. Serantoni, J. Clohessy and V. J. Cunnane, *Surf. Coat. Technol.*, 2004, **182**, 7–13.
48 A. I. Melato, M. H. Mendonça and L. M. Abrantes, *J. Solid State Electrochem.*, 2009, **13**, 417–426.
49 A. Rudge, J. Davey, I. Raistrick, S. Gottesfeld and J. P. Ferraris, *J. Power Sources*, 1994, **47**, 89–107.
50 G. Inzelt, M. Pineri, J. W. Schultze and M. A. Vorotyntsev, *Electrochim. Acta*, 2000, **45**, 2403–2421.
51 C. Bodart, N. Rossetti, J. Hagler, P. Chevreau, D. Chhin, F. Soavi, S. Brian Schougaard, F. Amzica and F. Cicoira, *ACS Appl. Mater. Interfaces*, 2019, **11**, 17226–17233.
52 J. Zhang, C.-Y. Hsu and M. Higuchi, *J. Photopolym. Sci. Technol.*, 2014, **27**, 297–300.
53 (*a*) P. M. S. Monk, R. J. Mortimer and D. R. Rosseinsky, *Electrochromism: Fundamentals and Applications*, VCH, Weinheim, 1995; (*b*) K. Bange and T. Gambke, *Adv. Mater.*, 1990, **2**, 10–16.
54 (*a*) W. Wei, W. Ye, J. Wang, C. Huang, J.-B. Xiong, H. Qiao, S. Cui, W. Chen, L. Mi and P. Yan, *ACS Appl. Mater. Interfaces*, 2019, **11**, 32269–32281; (*b*) W. Wei, J. Wu, S. Cui, Y. Zhao, W. Chen and L. Mi, *Nanoscale*, 2019, **11**, 6243–6253; (*c*) W. Wei, W. Chen, L. Ding, S. Cui and L. Mi, *Nano Res.*, 2017, **10**, 3726–3742.